

Interannual Variability of Thermal Conditions in the Kuroshio Energetically Active Zone and Adjacent Areas of the Philippine Sea

I. D. Rostov^{a*}, E. V. Dmitrieva^a, and N. I. Rudykh^a

^a*Il'ichev Pacific Oceanological Institute, Far Eastern Branch, Russian Academy of Sciences,
ul. Baltiiskaya 43, Vladivostok, 690041 Russia*

**e-mail: rostov@poi.dvo.ru*

Received November 17, 2020

Revised December 28, 2021

Accepted March 30, 2022

Abstract—Regional features and possible causal relationships of interannual changes in air temperature, sea surface temperature (SST), and water temperature in the upper 750-m layer with variations in atmospheric pressure, wind, heat fluxes on the ocean surface, and climate indices over the last four decades were determined. It is shown that in different regions of the Philippine Sea air temperature increased by 0.2–0.5°C and SST rose by 0.6–0.8°C. In several layers of the water column, there are multidirectional trends in water temperature. In winter, in the area of the Kuroshio energetically active zone of the ocean (EAZO), both maximum fluxes and trends in sensible and latent heat from the ocean to the atmosphere were recorded. The variations in air temperature and SST have stable correlations with variations in the zonal and meridional components of wind speed and climate indices.

DOI: 10.3103/S1068373922040057

Keywords: Kuroshio EAZO, Philippine Sea, climate change, air and water temperature, wind, heat fluxes on the ocean surface, trends, climate indices, correlation, regional features

INTRODUCTION

The areas of boundary currents on the western periphery of the Northern tropical and Northern subtropical gyres [10] situated in the Philippine Sea, play a major role in accumulating heat energy in the processes of transfer, redistribution of heat, and formation of regional and global climate conditions [8, 22]. Here, the ocean–atmosphere interaction processes intensify, heat and moisture fluxes to the atmosphere increase, and significant temperature anomalies are formed. Sensible and latent heat fluxes on the sea surface intensify in winter and play a key role in the climate system dynamics [18, 27].

This area is situated on the northern periphery of the Western Pacific warm pool (WPWP [25]), where sea surface temperature (SST) exceeds 28 °C, being the connecting link of water circulation in the tropical and middle latitudes. In the Pacific Ocean, the discharges of western trade currents increase from east to west, which favors the formation of increased heat energy reserves in the upper layer with a thickness of several tens of meters in the western equatorial-tropical zone. It was shown [25] that in the recent years the area, volume, and heat content of the WPWP have increased, and the parameters of its interannual anomalies indicate El Niño–Southern Oscillation events (phases NINO 3, NINO 3.4, NINO 4, SOI), Pacific Decadal Oscillation (PDO), and wind field variability. According to our estimates, there is a statistically significant trend in the equatorial Pacific trade wind index at the level of 850 hPa (PTW) in the analyzed period, and the average annual surface speed of eastern winds in the zone of 0–10°S, 160°E–160°W increased by 1.5 m/s per 40 years. At the same time, interannual variations in the zonal component of wind speed in this sector highly correlate with variations in the SST and water temperature in the subsurface layers in the area of the WPWP (the correlation coefficient $R \sim |0.7|$).

The study area is a part of the energetically active zone of the ocean and atmosphere in the Northwest Pacific, which has a major effect on the processes in both adjacent ocean areas and the Earth climate system. The main typhoon paths pass through it, and the cyclone activity affects the characteristics of the ther-

mal regime in the North Pacific [2, 29]. The cyclone activity over the Northwest Pacific and Far Eastern seas is mainly formed by tropical and western extratropical cyclones in the warm season and by active western and southern extratropical cyclones in the cold season [11].

The main tendencies in the interannual variations in thermal conditions in this region are determined by global climate changes, teleconnections in the ocean and atmosphere, the redistribution of heat between different parts of the World Ocean and are affected by El Niño/La Niña events, while decadal and longer changes are consistent with the PDO phases [1, 4, 19, 25, 33]. Teleconnections are considered as synchronous correlations, mainly between meteorological parameters in distant areas and play an important role in the global climate system [4]. The El Niño and La Niña events are the dominating factors of the natural cyclicity of climate variability on various timescales and were investigated rather well. They are associated with the phases of large-scale ocean surface heating and cooling in the central, eastern, and western equatorial Pacific in combination with changes in the atmospheric circulation, current fields, sea-level pressure gradient from east to west, wind, thermocline depth, and other characteristics [1, 17]. Pacific Decadal Oscillation is the dominant factor in the SST variability in the North Pacific. It is characterized by the alternation of warming and cooling phases in the west, within the Kuroshio–Oyashio and in the northeastern Pacific. The positive PDO phase is associated with the increasing wind impact and the extending subpolar gyre in the North Pacific and the deepening Aleutian Low [33].

As a result of anthropogenic impact under conditions of increasing greenhouse gases emission to the atmosphere, global warming continues. This process is accompanied by the reorganization of atmospheric processes, which leads to the redistribution of energy excess between the atmosphere and the ocean. About 90% of excessive heat added to the climate system is absorbed by the ocean [13]. At the same time, the thermal structure of the upper 100-m layer is basically determined by the surface heat budget, and the impact of advection and mixing of water is more significantly manifested in the subsurface layer [5].

The system of the main currents in the study area consists of the North Equatorial Current, Mindanao Current, Equatorial Counter Current, and Kuroshio current system consisting of the major current and its countercurrent, Luzon and Taiwan currents [3] (they are schematically presented in Fig. 1c). The Kuroshio is the key component of large-scale circulation in the system of western boundary currents, the major source of heat inflow to the atmosphere, and the peculiar modulator of climate change in adjoining areas, transporting the heat excess from low to middle and high latitudes [20, 27, 31, 32]. At the same time, the Kuroshio EAZO was distinguished as a separate area among five World Ocean EAZOs in the concept of the Sections national monitoring program performed in 1980s–1990s. In the present paper, this area is considered in the limits of the Kuroshio within the Philippine Sea. The significant interest to the investigation of the Kuroshio is confirmed by the examples of numerous national, international programs and complex expeditions such as MGG-MGS with participation of *Vityaz'* research vessel (Shirshov Institute of Oceanology, Russian Academy of Sciences), Cooperative Study of the Kuroshio and Adjacent Regions (CSK), Kuroshio Edge Exchange Processes Study (KEEP), “KISZ-80,” “KETI-82” (Far Eastern Research Hydrometeorological Institute), Sections, WOCE, etc. Since 1967, Japan Meteorological Agency (JMA) has provided routine surveys at the section along 137° E from 3° to 34° N twice a year and has carried out other expeditions in the Philippine Sea, which allowed accumulating a unique volume of information about the water structure and dynamics in the region [23, 28]. As a result of long-term studies in this region, rather complete oceanographic datasets were formed, and numerous studies were accomplished analyzing the spatiotemporal variability of the structure and dynamics of water and various climatic characteristics in different years. Since 1996, JMA has published regional yearbooks with the results of monitoring long-term changes in the atmospheric and oceanic characteristics in the area of the Japanese islands and Kuroshio as compared to global changes [19].

The objective of the present paper is to reveal trends and spatiotemporal features of interannual variations in air temperature, SST, water temperature in the upper 750-m layer, and separate climatic parameters in the study region, as well as to analyze their possible causal relationships with large-scale and regional processes in the ocean and atmosphere over the last four decades, i.e., at the modern stage of global warming. Regional features and quantitative characteristics of long-term interannual trends in pressure, wind, and heat fluxes on the ocean surface, surface air temperature, SST, and heat content of the water column, which are studied using the set of observational data, modern assimilation models, and reanalysis, are underestimated. It is also necessary to determine the statistical significance and interrelations of these changes with the phases of predominant modes of the natural cyclic variability of climatic characteristics under conditions of increasing anthropogenic impact in such specific area with high thermodynamic activity as the Kuroshio EAZO.

DATA AND METHODS

This research used observational data on air temperature from 39 weather stations of the GHCN-M (V3) NOAA global climate network (<https://www.ncdc.noaa.gov/ghcnm/v3.php>) over the period from 1978 to 2019, NCEP/NCAR Reanalysis-1 surface air temperature (T_a) data [24], fields of pressure, wind, and heat fluxes on the ocean surface, the series of climate (circulation) indices [6] (PDO, AMO, SOI, NP, WP, PNA, PTW, EP/NP) taking into account their seasonality. The listed data were taken from <https://psl.noaa.gov/data/gridded/index.html> (the developer is NOAA/ESRL/Physical Sciences Laboratory (PSL), Boulder, USA), <https://www.nodc.noaa.gov/> and <https://www.cpc.ncep.noaa.gov/> (NOAA/NCEI/CPC). The interannual changes in water temperature were analyzed using the data of optimum SST interpolation (NOAA OI SST V2) for 1982–2019 from <https://www.esrl.noaa.gov/psd/> [30] and data on water temperature (T_w) and current velocity at different levels from the GODAS system [16] (<https://www.esrl.noaa.gov/psd/data/gridded/data.godas.html>) for 1980–2019. In addition, data of JMA long-term oceanographic surveys in the Philippine Sea were applied [23].

The statistical characteristics (mean, variance, anomalies, correlation coefficient, trends for different seasons) were calculated, and the decomposition of the fields of anomalies of the characteristics to principal components of empirical orthogonal functions (EOFs) was carried out using the single technique [9]. Taking into account the duration of the summer and winter monsoons and the intraannual variations in T_a and SST, the conditionally warm or summer (June–September) and conditionally cold or winter (November–March) seasons (periods) were distinguished. The trends were estimated for the average annual and seasonal values of the parameters and their anomalies (Δ). The anomalies were determined as a deviation from the mean for all years of the 30-year period (1984–2013).

REGIONAL FEATURES OF INTERANNUAL VARIABILITY OF AIR TEMPERATURE AND SST

Based on three principal components of the EOF for the SST anomaly (SSTA) field in winter (when horizontal temperature gradients are increased, and three principal components describe 80% (50% + 25% + 5%) of SSTA variability) three relatively isolated areas were distinguished in the sea: northern (N), central (C), and southern (S) (see Fig. 1g). Their location is generally consistent with the natural physiographic zones of the sea area and with the schemes of spatial features of the circulation characteristics of sea water [3, 10, 28]. In the northern area, the Kuroshio current is situated, the central area is the western periphery of the North Pacific subtropical gyre, and the southern area is located on the western periphery of the North Pacific tropical gyre, within the WPWP [25]. The 28 °C isotherm of average annual SST values passes along the northern boundary of the southern area in the zone of 15–18 °N. Climatic differences between the distinguished areas are manifested from the comparison of both generalized estimates of the mean and extreme values of air temperature and SST variations (Table 1) and their trends (Fig. 1). In all areas, the mean and extreme estimates of SST are higher than for T_a . These estimates naturally increase from north to south, and the variance increases in the opposite direction, reaching the maxima in the northern area in the cold season. According to the observations at the coastal and island stations and the reanalysis, the maximum values of T_a and SST were registered in 1998 in the northern and central areas and in 2010 and 2017 in the southern area. In the second half of 1997–the beginning of 1998 as well as during the similar periods in 2009–2010, El Niño intensified [26], and in the spring of 2008 and in the summer of 2010, the La Niña phase began (https://www.data.jma.go.jp/gmd/cpd/data/elnino/learning/faq/elnino_table.html, <https://ds.data.jma.go.jp/tcc/tcc/products/elnino/ensoevents.html>). According to the same JMA monitoring data, only the La Niña phase was recorded in the second half of 2017, during which the strengthening of trade winds leads to the decrease in T_a and SST in the eastern equatorial Pacific and to their increase in the western part. The greatest contribution to the formation of the maxima in the interannual variations of average annual T_a and SST in all areas in the mentioned years (Table 1) is made by the warm-season months during La Niña.

In the presence of high correlation between variations in air temperature and SST, the trends and basic features of the spatial distribution of the trends in T_a and SST are consistent with each other and characterized only by the positive values of the trends (b) in the average annual values of temperature. The ranges of their maximum values ($b = (0.2–0.3) \text{ } ^\circ\text{C}/10 \text{ years}$) are concentrated in the northern and southern areas of the sea (Figs. 1a and 1b). In the warm season, the distribution of the trends in SST (which is a more persistent characteristic than T_a) within the entire sea is more uniform than for T_a , and there are zones with negative values of b in the field of T_a . The results of estimating the trends using instrumental observations at weather stations demonstrated in Fig. 1b are in satisfactory agreement with reanalysis data. The EOF prin-

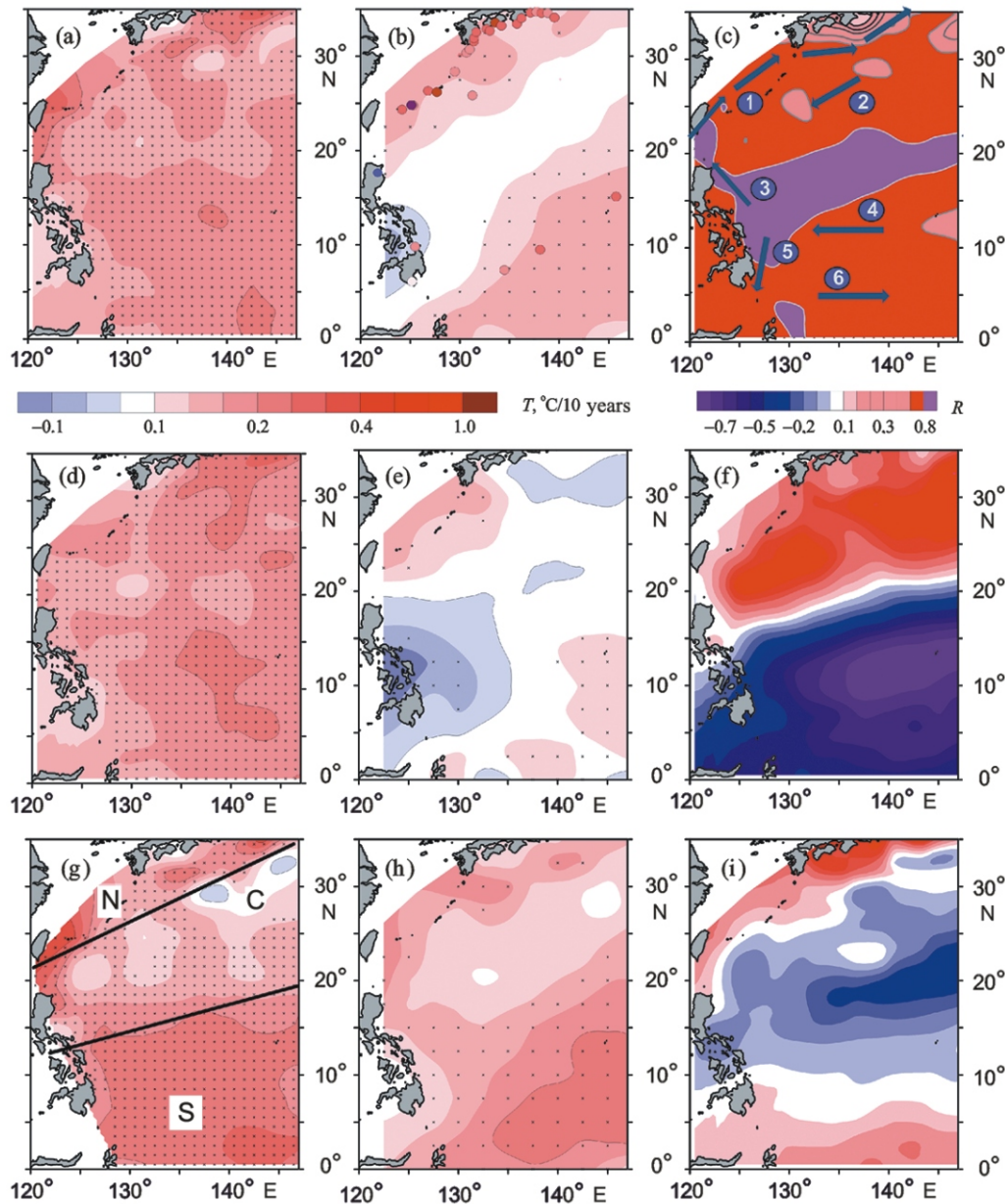


Fig. 1. The linear trends ($C/10$ years) in the anomalies of (a, d, g) sea surface temperature and (b, e, h) air temperature: (a, b) the average annual trend, for (d, e) the warm and (g, h) cold seasons in 1982–2019, as well as the distribution of coefficients of (c) the first, (f) second, and (i) third EOF modes for the interannual SSTA variations in the cold season. Figure (g) presents the location of the distinguished areas, figure (b) shows the value of T_a anomalies at weather stations, figure (c) demonstrates the scheme of the major currents: (1, 2) Kuroshio and its countercurrent, (3) Luzon Current, (4) North Equatorial Current, (5) Mindanao Current, (6) Equatorial Counter Current. The crosses mark the grid points where the trend estimates are statistically significant at the 95% level.

incipal components carry important information about the main modes of large-scale interannual variability of the SSTA field, whose features can be evaluated using the variance, trends at grid points, and connectivity of variations in the spatial coordinate system. The first three SSTA EOF modes C1–C3 accumulate 80% of variance of interannual variations in the anomalies of average annual SST in the region. The distribution of the SSTA EOF coefficients C1 both in the warm (Fig. 1c) and cold seasons is represented by the positive values and characterizes the synphase variations in the SSTA in the whole basin. In the sea area, the positive interannual trends in the SST are clearly pronounced, while trends in T_a are mainly observed in the cold season (Table 2). The distribution of the coefficients of the second SSTA EOF mode reflects the anti-phase

Table 1. The mean and extreme values of average annual air temperature (°C; 1978–2019) and SST (°C; 1982–2019) in the distinguished areas

Parameter	Area		
	Northern	Central	Southern
T_a			
Mean	19.02	24.91	27.57
Max	20.10 (1998)	25.79 (1998)	27.88 (2010)
Min	18.17 (1984)	24.52 (1996)	26.76 (1992)
σ^2 (year)	0.16	0.07	0.06
σ^2 (warm)	0.14	0.04	0.03
σ^2 (cold)	0.40	0.24	0.21
SST			
Mean	23.40	26.18	29.06
Max	24.37 (1998)	26.94 (1998)	29.58 (2017)
Min	22.78 (1982)	25.69 (1984)	28.50 (1991)
σ^2 (year)	0.14	0.11	0.07
σ^2 (warm)	0.16	0.10	0.09
σ^2 (cold)	0.19	0.16	0.13
<i>R</i>	0.79	0.88	0.79

Max, min are the maximum and minimum values, the year is given in brackets; σ^2 is variance over different periods; *R* is the coefficient of correlation between the average annual values of T_a and SST in the distinguished areas. Here and in the other tables, statistically significant (95%) estimates are bolded.

Table 2. The pattern and interannual trends in the climatic parameters in different areas of the Philippine Sea over the last four decades

Area	Parameter	<i>b</i>	tr	<i>D</i>	b_w	b_c
Northern	T_a	0.13	0.5	13	0.07	0.16
	SST	0.19	0.8	30	0.19	0.18
	<i>U</i>	0.0	0.0	0	0.09	-0.02
	<i>V</i>	0.08	0.3	12	0.17	0.01
	<i>LH</i>	5.21	20.8	41	2.74	9.60
	<i>SH</i>	0.69	2.8	4	0.08	1.96
Central	T_a	0.04	0.2	3	0.01	0.09
	SST	0.14	0.6	23	0.16	0.13
	<i>U</i>	-0.02	-0.1	0	0.0	-0.08
	<i>V</i>	0.04	0.2	2	0.04	-0.01
	<i>LH</i>	2.91	11.6	26	5.46	3.14
	<i>SH</i>	0.85	3.4	23	0.97	1.15
Southern	T_a	0.10	0.4	20	0.02	0.18
	SST	0.17	0.7	51	0.18	0.20
	<i>U</i>	0.01	0.0	0	-0.04	0.0
	<i>V</i>	-0.02	-0.1	3	-0.10	0.04
	<i>LH</i>	1.33	5.3	12	1.89	1.53
	<i>SH</i>	0.49	2.0	27	0.95	0.24
Entire sea	T_a	0.08	0.3	17	0.02	0.12
	SST	0.16	0.6	46	0.17	0.17

b is the linear trend slope coefficient, °C per decade; tr is the trend per 40 years, °C; *D* is the trend contribution to total variance, %; b_w , b_c are the trend coefficients for the warm and cold seasons, respectively; *LH* and *SH* are the latent and sensible heat fluxes, W/m²; *U*, *V* are the zonal and meridional wind speed components, m/s.

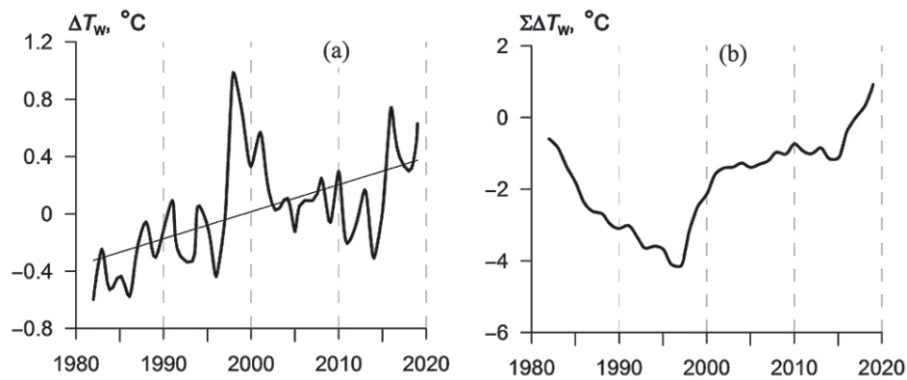


Fig. 2. The interannual changes in (a) the anomalies and (b) accumulated anomalies of average annual SST in the northern area.

SST variations in the northern and southern parts of the sea (Fig. 1f), and the distribution of the third mode indicates similar variations in three distinguished areas (Fig. 1i).

In general, over the recent 40 years, air temperature in different regions increased by 0.2–0.5 °C and SST rose by 0.6–0.8 °C, and the maximum growth was observed in the northern part of the sea. On average for the sea, the contribution of the trend to total variance of fluctuations in T_a and SST made up 17 and 46%, respectively. As noted above (Table 1), the maximum in 1998 is pronounced in the temporal variations in the average annual T_a and SST in the northern and central areas (Fig. 2a), which is also distinguished in the distribution of temporal coefficients of the first SSTA EOF mode. Then, until the mid-2010s, the SST anomalies were decreasing. This period was considered as a hiatus of the global warming (Fig. 2a), in particular, in the area of the Kuroshio and adjoining regions [32, 34]. In the southern area, the 1998 maximum and the subsequent hiatus against a background of the general positive trend are not strongly pronounced. In this area in the cold seasons of 1991–1993 there were significant negative anomalies of interannual values of T_a (to –2.4 °C) and SST (to –0.8 °C), which could be associated with an increase in the average speed of northern winds in December 1992 (up to 3.6 m/s as compared to the normal equal to 2.2 m/s). At the same time, the northern boundary of the WPWP (the 28 °C isotherm) moved to the south, and the average annual sensible heat flux from the ocean to the atmosphere reached the maximum of 10.7 W/m² in 1992.

CORRELATION BETWEEN THERMAL CONDITIONS AND ATMOSPHERIC PROCESSES

The following changes occurred in the wind characteristics (Table 2). During the summer monsoon, statistically significant trends towards the strengthening of southern winds by 0.7 m/s were observed in the northern area, while the trends towards their weakening by 0.4 m/s were registered in the southern area. In winter, no significant trends in the zonal and meridional wind speed components were found. At the same time, the variations in T_a and wind speed components are characterized by the moderate correlation ($R = 0.4–0.6$) both in summer and winter.

The differences in the pattern of warming in the separate areas are significantly determined by local conditions, by the value of advective transport of heat by currents, as well as of sensible (SH) and latent (LH) heat of condensation in the atmosphere [18, 29, 33]. As known, the area of the Kuroshio EAZO plays an important role in the accumulation of heat energy and heat transfer to neighboring areas. This is confirmed by the quantitative estimates of heat exchange at the ocean–atmosphere interface and by their trends under global warming. The values of heat fluxes (W/m²) on the ocean surface are given below for different areas of the Philippine Sea (N, C, and S) and the adjacent western subarctic (WSA) sea area: average annual (M), warm- (W) and cold-season (C) ones on average for 1980–2019:

Area	Northern			Central			Southern			WSA		
	M	W	C	M	W	C	M	W	C	M	W	C
Period												
SH	45	7	88	18	5	33	8	7	10	15	5	25
LH	167	90	246	146	108	198	117	111	130	42	12	71

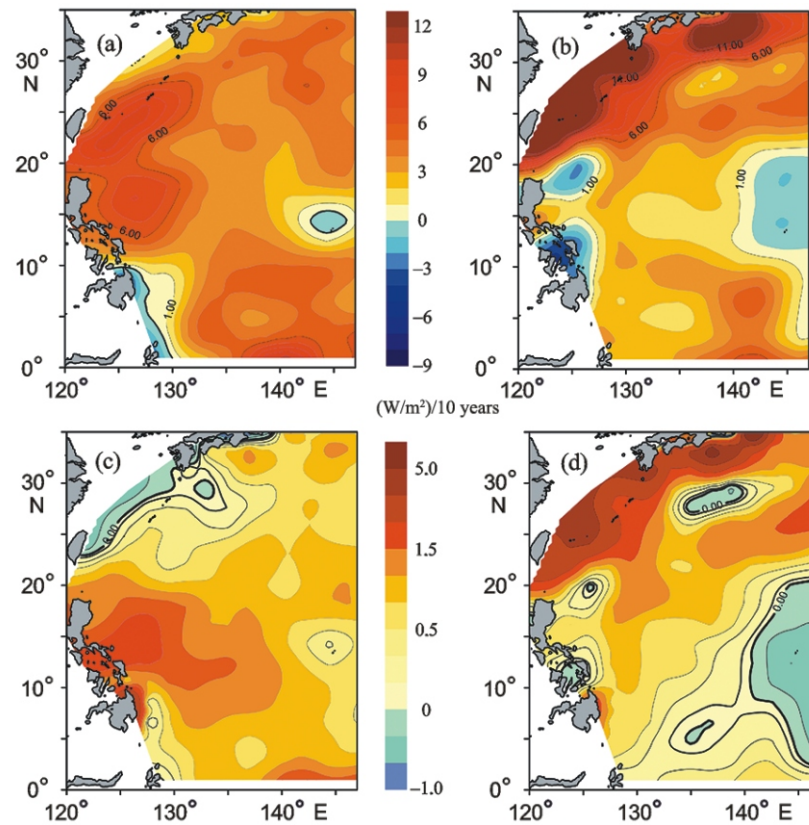


Fig. 3. The trends in (a, b) latent and (c, d) sensible heat for (a, c) the warm and (b, d) cold seasons in 1980–2019.

The maximum values of average annual heat fluxes from the ocean to the atmosphere are localized in the northern area (in the Kuroshio EAZO) and observed in the cold season. The fluxes LH significantly exceed the fluxes SH , which is also typical of the outgoing part of heat budget in the low-latitude areas. For comparison, the values of LH in the adjoining area of the western subarctic are several times smaller. There are statistically significant trends in the interannual variations in LH and SH in most of the sea area (Fig. 3). In the northern area in some winter months, the fluxes LH and SH reached 380 and 170 W/m^2 , i.e., the highest values for the whole Pacific area, and increased at a rate up to 10–15 and 5–8 W/m^2 per decade, respectively, at the turn of the 20th and 21st centuries. Excessive heat comes to the atmosphere and is transferred to the neighboring areas. The interannual changes in the fluxes of heat coming to the atmosphere in the northern and central areas of the Philippine Sea and the variations in water temperature and air temperature in different areas of the subarctic Pacific are characterized by moderate correlations ($R = 0.3–0.6$). Under the influence of different mechanisms of small-scale turbulence and density convection, SST variations in these areas are transferred to deeper layers.

TEMPERATURE VARIABILITY IN THE SURFACE AND INTERMEDIATE LAYERS

The interaction between separate links of the system of currents and water masses of various origin are a reason for the formation of the complex spatial structure and various-scale variability of thermohaline characteristics in the Kuroshio EAZO and adjoining areas of the Philippine Sea. Positive phases and trends in the PTW and SOI indicating the strengthening of trade winds were accompanied by a certain increase in the velocity of the North Equatorial Current, Kuroshio, and heat advection from the WPWP [25, 28, 31]. Inhomogeneities in the horizontal and vertical structure of flows, the vortex generation and meandering create conditions for the intrusion of isolated water volumes in different layers, which leads to the thermocline erosion, an intensification of vertical exchange, and an increase in the heat fluxes from the ocean to the atmosphere [20, 27]. Under conditions of the closed annual cycle, the exceeding of the heat emission through the ocean surface over its influx is compensated by the advection of heat by currents [5].

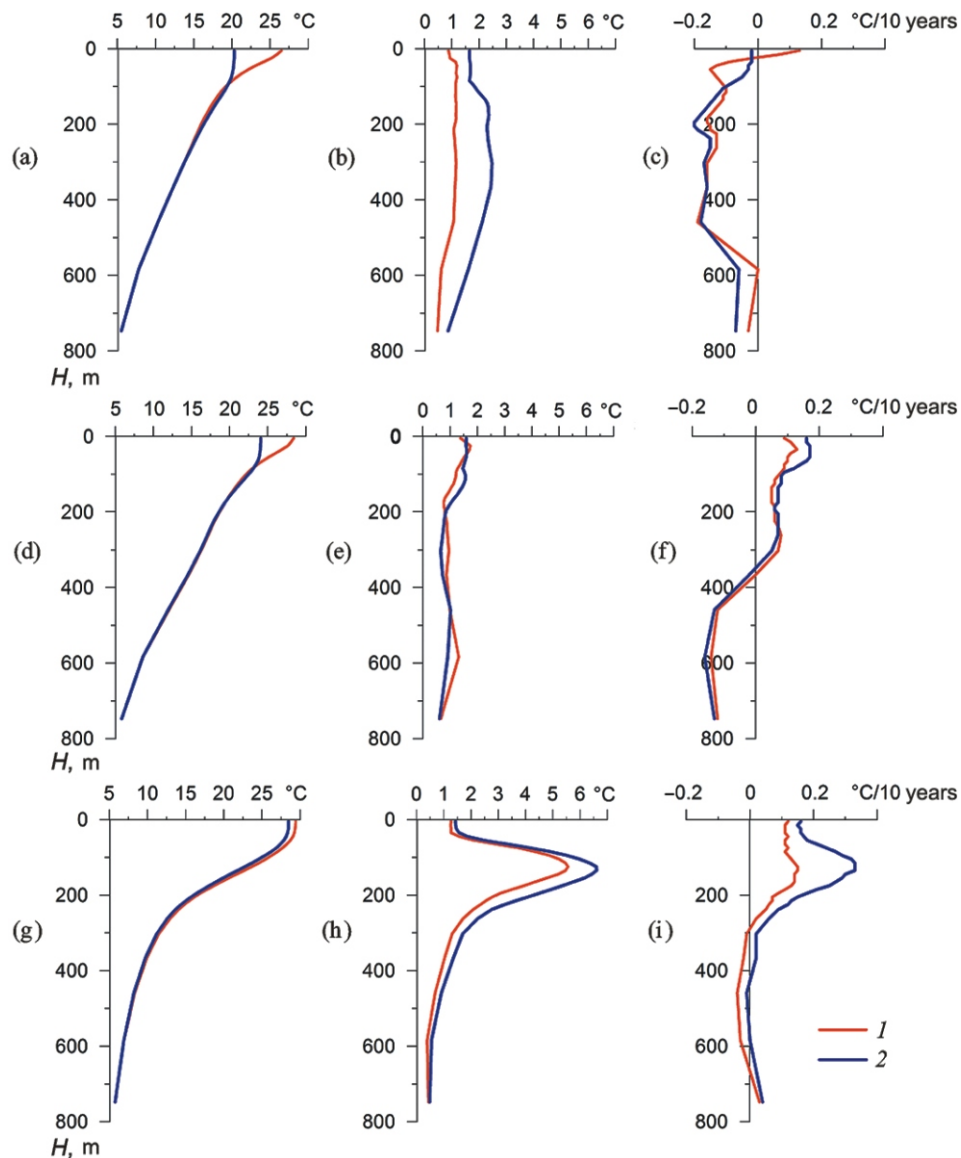


Fig. 4. The vertical distribution of (a, d, g) average annual water temperature T_w , (b, e, h) the difference between the maxima and minima of T_w , and (c, f, i) the value of linear trends in T_w for 1980–2019 in (1) the warm and (2) cold seasons in different areas of the Philippine Sea according to the GODAS data: in (a, b, c) the northern, (d, e, f) central, and (g, h, i) southern areas.

Data of the 50-year cycle of repeating observations at the section along 137° N in the Philippine Sea [23, 28] and GODAS [16] allow monitoring interannual trends in water temperature (T_w) at different horizons in the distinguished areas. Like the variations in T_a and SST, they are manifested in the alternation of warm and cold periods and in the formation of separate layers and zones with temperature trends of various magnitude and sign. These processes are highly inhomogeneous in time and space [14]. For example, water temperature in the upper and intermediate layers in the northern and southern areas of the mentioned section was above the normal in 1975, whereas it was below the normal in 2017 [19]. The sign, magnitude, and statistical significance of the interannual trend in T_w noticeably differed in separate layers and areas of the sea [28]. Therefore, the characteristics of variability in the vertical structure of the temperature field averaged within each of the three areas are considered below (Fig. 4). The highest amplitudes of variations in T_w are observed in the southern area of the sea in the upper thermocline layer, and the smallest ones are registered in the central area. The values of the trends in T_w in the surface layer and SST are close. The sign and magnitude of the temperature trends in separate layers of the water column highly vary with depth. In the northern area, where, as shown above, the maximum sensible and latent heat fluxes from the ocean to the

atmosphere were recorded, there are negative temperature trends and the cooling within the whole layer, except for a thin surface layer (in summer). At the same time, in the central area multidirectional trends are clearly pronounced: toward the warming in the upper 350-m layer and toward the cooling in the underlying layers. In the southern area, a gradual accumulation of heat in the upper 300–400-m layer is mainly observed, its trends are more pronounced in the cold season; in summer, the heat loss is observed in the layer of 300–700 m. The analysis of data on the correlation between the interannual changes in T_w at different depths and the variations in air temperature and wind speed revealed that statistically significant correlations between these parameters are observed to the depth of 50, 200, and 200–300 m in the northern, central, and southern areas, respectively. The reasons and mechanisms of the cooling and warming processes in individual water layers are a subject of special research involving reliable data on the structure and dynamics of water in the region.

RELATIONSHIPS BETWEEN THE VARIABILITY OF AIR TEMPERATURE, SST, WIND, AND CLIMATE INDICES

The relationships characterizing the influence of different circulation mechanisms and large-scale pressure and temperature anomalies in the ocean and atmosphere on the regional features of interannual variations in water temperature, air temperature, and other climatic characteristics are complex and diverse even within one sea area. The spatial features of the distribution of regression coefficients (*Reg*) of interannual variability both for the SSTA and the first three SSTA EOF modes (C1–C3) for the Philippine Sea and 500 hPa geopotential height anomalies (AH_{500}) over the North Pacific were analyzed to reveal the structure of these connections (Fig. 5). The variations in H_{500} in the middle troposphere highly correlate with the state of the atmospheric centers of action, with changes in the corresponding climate indices, temperature and wind characteristics. The spatial distribution of the AH_{500} EOF C1 in the warm season, as well as of the SSTA EOF C1 in both seasons (Fig. 1c), is characterized by the synphase changes within the whole sea area. In the warm season, the values of the SSTA trends (Fig. 1d) and regression coefficients of variations in the AH_{500} and SSTA C1 are positive and statistically significant for the whole sea (Fig. 5a). In the cold season, when the dipole (north–south) pattern of antiphase variations in this AH_{500} EOF mode is formed over the North Pacific, the negative values of *Reg* (–0.1...–0.3) were observed in the northern and central areas of the Philippine Sea, while the positive values (0.4–0.6) were recorded in the southern area (Fig. 5b). The zone of the maximum values spreading from west to east to 140°W is pronounced in the spatial distribution of the second AH_{500} EOF mode over Japan and the northern Philippine Sea during a year (Figs. 5c and 5d). This zone may be connected with the latitudinal zone of the East Asian mid-tropospheric jet stream resulting from the formation of upper-air frontal zones with high horizontal temperature gradients [12]. The speed and frequency of jet streams are maximal in the zone of 25°–35°N and reach the highest values in the vicinity of 30°N, 120°–140°E. In summer, the axis of jet streams moves to the north, and their velocities have generally decreased in the recent decades [12]. The decrease in the jet stream speed is consistent with a general trend toward a decrease in the Western Pacific index (WP) [7, 9], indicating the weakening of the zonal transport in the atmosphere. On the maps of the distribution of regression coefficients for the second AH_{500} and SSTA mode (C2) in the cold season (Fig. 5d) in the central and northern areas of the Philippine Sea, there is a zone of statistically significant values of *Reg* (0.4–0.5), which spreads further to the east beyond the sea up to 150°W and moves to the north in the warm season (Fig. 5c). The corresponding regression coefficients for the variations in the AH_{500} C3 (which indicates ~12% of contribution to the variability of AH_{500}) and SSTA C3 in most of the sea area, are negative in the warm season and small in the cold season (–0.2...0.2). The revealed correlations and regressions reflect the features of the spatiotemporal structure of the main variability modes of the SSTA, atmospheric circulation characteristics, and the state of the atmospheric centers of action, which may be generally expressed in terms of climate indices [6]. Below see the estimates of the respective coefficients of correlation between SSTA, SSTA EOF C1–C3, and AH_{500} C1–C3 for the warm and cold (in brackets) seasons.

Parameter	AH_{500} C1	AH_{500} C2	AH_{500} C3
SSTA	0.7 (0.2)	0.3 (0.4)	–0.3 (0.0)
SSTA C1	0.7 (0.2)	0.2 (0.5)	–0.3 (0.0)
SSTA C2	–0.2 (–0.6)	0.4 (0.3)	0.1 (0.4)
SSTA C3	–0.1 (0.2)	–0.4 (0.0)	0.1 (0.2)

There is an effect of the first (in summer) and second (in winter) modes of AH_{500} variations on the SSTA field characteristics both for the entire Philippine Sea (the second line) and for its separate modes describing the spatiotemporal pattern of SSTA variations.

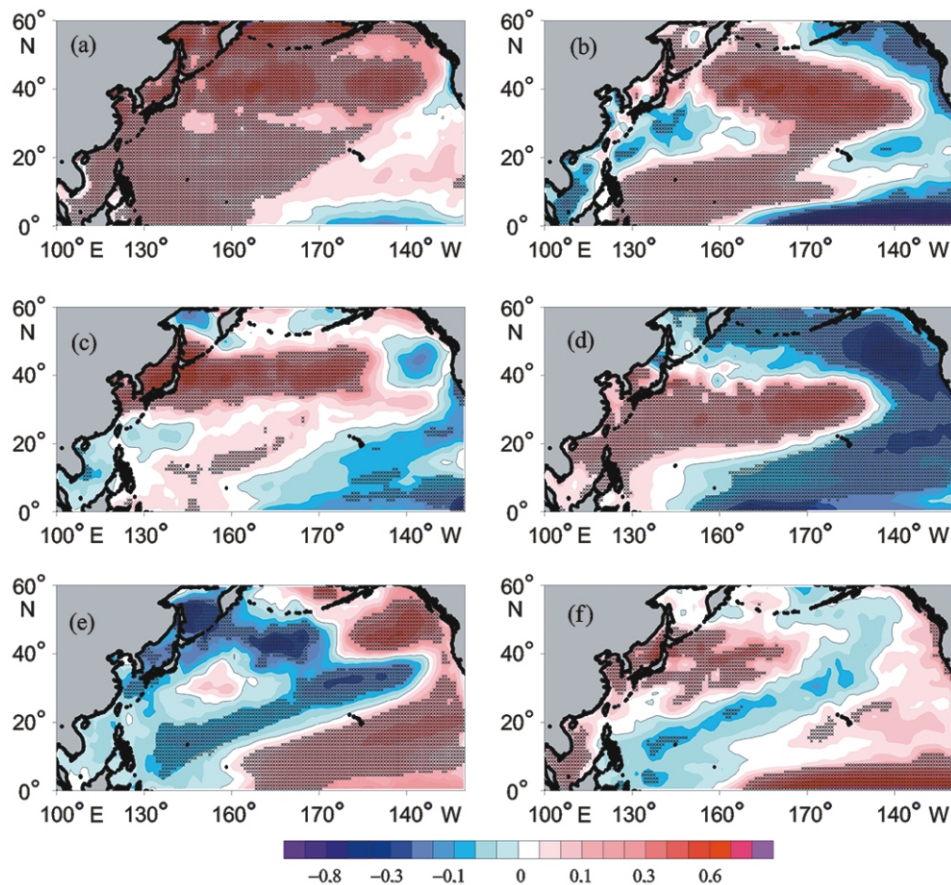


Fig. 5. The coefficients of linear regression Reg of SST variations with the first three H_{500} geopotential height anomaly EOF modes (a, b) C1, (c, d) C2, and (e, f) C3 in (a, c, e) the warm and (b, d, f) cold seasons. Here and in Fig. 6, the crosses mark the grid points where the estimates are statistically significant at the 95% level.

As noted above, the relationships characterizing the influence of different circulation mechanisms and large-scale pressure and temperature anomalies in the ocean and atmosphere on the regional features of interannual variations in climatic parameters are complex and diverse. The large-scale processes that influence and form a background for regional hydrometeorological conditions development, can be characterized by a number of climate indices that are commonly used in modern climate change research. Climate indices are used as indicators of large-scale climatic processes and teleconnections between them [4, 6]. The relationships between the features of the spatiotemporal variability of thermal conditions and the wind field in the study area with the following climate indices are most clearly manifested: Western Pacific (WP), Southern Oscillation (SOI), Atlantic Multidecadal Oscillation (AMO), Pacific Trade Wind (PTW), East Pacific/North Pacific (EP/NP) (Table 3).

As follows from the table, the processes in the ocean and atmosphere corresponding to these climate indices take part in the formation of the structure of the first three SSTA EOF modes, especially of the first (the most energetic) one or only the first one (AMO and EP/NP). In addition, the connections of the fields of temperature and wind with variations in the PDO and Okhotsk High index (OKH) are also pronounced in the area of the Kuroshio EAZO, and the connections with the Asian Low index (AD) are pronounced in the southern area. In some areas in the cold season, there are also statistically significant correlations of the variations in the North Pacific (NP) and Pacific/North American (PNA) indices, the values of the surface pressure difference between the Siberian High and Aleutian Low (SM-AL) with SST, T_a , and wind speed components. The formation of the second mode (C2) describing the anti-phase variations in SST and T_a in the northern and southern areas of the sea in winter is associated with the NP, WP, SOI, PTW, and PNA. In the formation of the characteristics for the third SSTA EOF mode (C3), there are connections with the PDO, SOI, PTW, and AD with account of their seasonality. The pattern and statistical significance of connections between the parameters of large-scale climatic processes and SSTA are indicated by the maps of regressions between SSTA and different climate indices (Fig. 6).

Table 3. The coefficients of correlation between interannual variations in the climate indices and variations in air temperature and water temperature in the distinguished areas, wind speed components, and coefficients of time series of the first SSTA EOF modes (C1–C3) for the warm and cold (in brackets) seasons

Area	Parameter	WP	SOI	AMO	PTW	EP/NP
N	b	-0.3 (0.1)	0.1 (0.4)	0.1 (0.1)	0.4 (0.9)	-0.2 (-0.1)
	T_a	0.0 (0.8)	0.3 (-0.2)	0.4 (0.3)	0.3 (-0.1)	-0.1 (-0.2)
	SST	-0.2 (0.6)	0.4 (0.1)	0.6 (0.6)	0.5 (0.4)	-0.3 (-0.3)
	V	0.0 (0.5)	0.1 (-0.4)	0.4 (0.0)	0.2 (-0.4)	0.0 (0.2)
	U	-0.3 (-0.6)	0.0 (0.1)	0.4 (0.0)	0.0 (0.1)	0.0 (0.4)
C	T_a	-0.2 (0.8)	0.2 (0.0)	0.3 (0.3)	0.2 (0.2)	-0.2 (-0.4)
	SST	-0.4 (0.7)	0.3 (0.1)	0.6 (0.5)	0.4 (0.4)	-0.4 (-0.3)
	V	0.1 (0.5)	0.4 (0.1)	0.3 (0.0)	0.2 (-0.4)	-0.1 (0.2)
	U	-0.3 (-0.4)	0.0 (-0.5)	0.0 (0.0)	0.1 (-0.2)	-0.2 (-0.5)
S	T_a	-0.2 (0.0)	0.5 (0.6)	0.4 (0.5)	0.5 (0.7)	-0.4 (-0.3)
	SST	-0.4 (0.0)	0.7 (0.8)	0.7 (0.5)	0.7 (0.9)	-0.4 (-0.2)
	V	0.2 (0.0)	-0.7 (0.5)	-0.5 (0.1)	-0.7 (0.7)	0.3 (-0.3)
	U	0.1 (-0.2)	-0.8 (0.0)	-0.3 (0.0)	-0.8 (-0.4)	0.2 (0.3)
Entire sea	C1	-0.4 (-0.4)	0.5 (0.5)	0.7 (0.6)	0.6 (0.7)	-0.4 (-0.3)
	C2	0.2 (0.6)	-0.2 (-0.6)	0.1 (0.0)	-0.2 (-0.5)	0.0 (-0.2)
	C3	-0.1 (-0.1)	-0.4 (0.2)	-0.1 (0.2)	-0.4 (0.1)	0.2 (-0.1)

b is the linear trend coefficient for the climate indices in 1979–2018.

In the interannual changes in the WP, there were positive trends in the cold season and statistically significant negative trends during the warm season. The strengthening of the positive or negative phase of the WP variations means zonal or meridional fluctuations in the position and intensity of the East Asian jet stream [12], as well as the strengthening or weakening of zonal and meridional transport in the atmosphere [15] and related changes in the wind and temperature regimes. Statistically significant connections between variations in this parameter and the changes in the wind speed components U and V are manifested only in the cold season in the northern and southern areas of the Philippine Sea. The processes parameterized by this index are associated with the first SSTA (and T_a) EOF mode in both seasons (Table 3). In the cold season, the pattern of the relationship between variations in the SSTA and the climate index changes (Fig. 6b), and it is determined by the features of the spatial structure of the second SSTA EOF mode (Table 3, Fig. 1f).

The SOI used for the regression analysis with the SSTA is a measure of the sea-level pressure (SLP) drop in the Pacific Ocean, from Tahiti in the southeast to Darwin (Australia) in the west. The SOI is used for monitoring and forecasting changes both in the El Niño–Southern Oscillation phenomenon and in the Walker circulation spreading across the whole tropical Pacific Ocean, the lower branch of which covers trade winds blowing from east to west. The Southern Oscillation is at the negative phase during El Niño and at the positive phase during La Niña (<https://ds.data.jma.go.jp/tcc/tcc/products/elniño/ensoevents.html>). The transition of interannual SOI variations to the positive phase corresponding to the increasing SLP difference between the mentioned regions, the strengthening of eastern trade winds in the Western Pacific and their weakening in the Eastern Pacific were observed during the analyzed period. At the same time, the SLP rise was due to a statistically significant positive trend in this parameter in the area of Tahiti (<https://www.cpc.ncep.noaa.gov/data/indices/tahiti>). The variations in the SOI and PTW are characterized by high correlation ($R = |0.7–0.9|$ depending on a season). An increase in the speed of eastern trade winds in the Western Pacific is accompanied by the advection of heat to the WPWP and the Philippine Sea. At the same time, the maps of regression dependences of the SSTA on the SOI and PTW are almost identical (Figs. 6c, 6d, 6e, and 6f), and the respective connections with the main SSTA EOF modes are similar (Table 3).

The index of the Interdecadal Pacific Oscillation (IPO), which was called the tripole index (TPI) for the IPO, is connected with three major centers of SSTA and air pressure variations on decadal timescales [21], as well as with the changes in the PDO and SOI affecting not only regions in America, East Asia, Australia, and New Zealand but also the global surface air temperature. Its value is based on the difference between the average values of the SSTA in the central equatorial part and in the northwestern and southwestern Pacific. In general, the alternation of the positive and negative phases of this process with a gradual transition of the IPO trend to the negative values has been observed since the mid-20th century. The positive phase

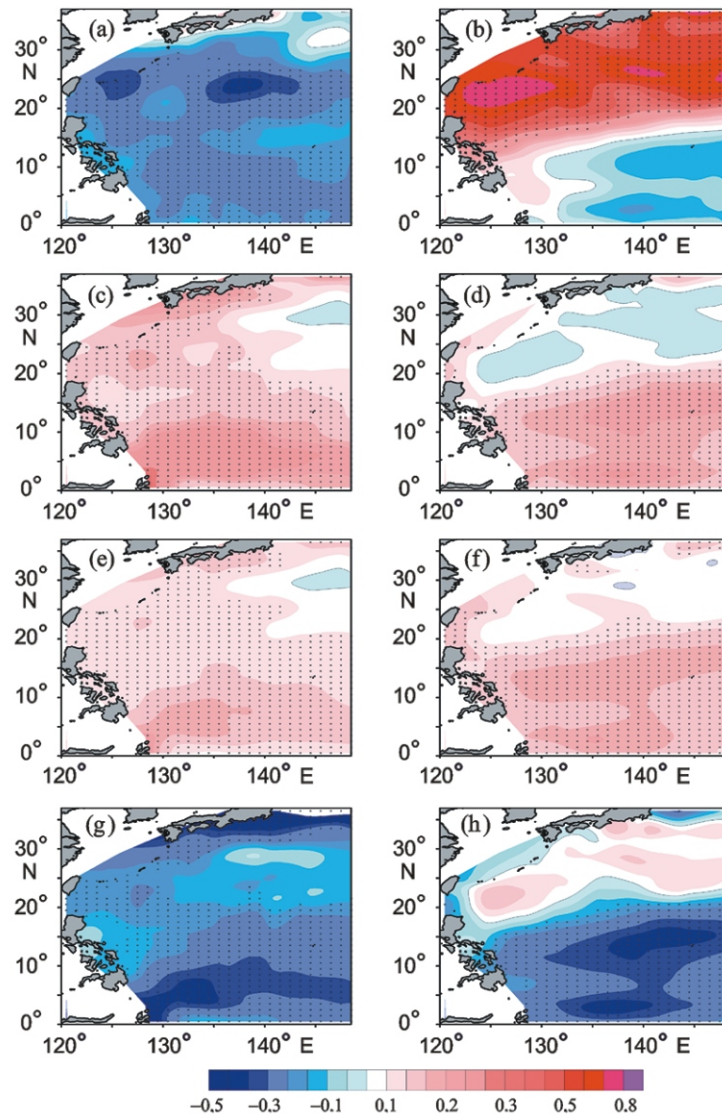


Fig. 6. The coefficients of linear regression Reg of SST variations with the climate indices: (a, b) WP, (c, d) SOI, (e, f) PTW, and (g, h) IPO in (a, c, e, g) warm and (b, d, f, h) cold seasons.

prevailed in 1977 to 1999, and the negative phase dominated in 1999 to 2012. At the same time, the negative IPO phase corresponds to the trend toward a transition to relatively higher sea-level pressure in the Central and East Pacific and to lower pressure in the Western Pacific, with the opposite trend during the positive IPO phase [21]. The IPO correlates with the formation of the structure of the first and second T_a and SSTA EOF modes (Figs. 1c and 1f), mainly in the cold season. A decrease in this index was accompanied by the increase in T_a and SST in the entire Philippine Sea.

In the northern area in different seasons, statistically significant correlations between variations in water temperature at different horizons and climate indices are pronounced in the upper quasihomogeneous layer and seasonal thermocline layer. These connections in the central and southern areas are observed to the depth of 200–350 and 350–700 m, respectively. The detailed analysis of the reasons and mechanisms of these relationships will be possible as soon as data are accumulated and can be an issue of further research.

CONCLUSIONS

The Philippine Sea is the major accumulator of heat energy, and the Kuroshio EAZO is the powerful source of heat for adjacent areas. In the area of the Kuroshio EAZO in winter, there are the greatest latent and sensible heat fluxes in the North Pacific with a value up to 380 and 170 W/m², respectively, which in-

crease at a rate up to 10–15 and 5–8 W/m² per decade. The interannual variations and trends in these fluxes in the northern and central Philippine Sea are consistent with changes in surface air temperature, SST, and water temperature in the surface and intermediate layers in different areas of the subarctic Pacific.

The interannual variability of average annual air temperature and SST in the area of the Philippine Sea is characterized by the positive values of trends b . The zones of maximum trends in average annual T_a and SST ($b = 0.2\text{--}0.3$ C/decade) were registered in the northwestern and southeastern sectors of the sea. In general, over the last 40 years, air temperature in the study area rose by 0.2–0.5 C and the SST increased by 0.6–0.8 C, the maximum growth was recorded in the northern part of the sea. The changes in T_a and SST are characterized by the significant correlation with variations in the zonal and meridional wind speed components and climate indices.

The highest amplitudes of interannual variations in T_w at different depths are observed in the southern area of the sea in the upper thermocline layer, and the smallest amplitudes are registered in the central area. The sign and magnitude of temperature trends at separate horizons vary quasynchronously and essentially differ in separate layers. In the northern area (the Kuroshio EAZO), where the maximum sensible and latent heat fluxes are registered, there are negative temperature trends and the cooling within the whole 750-m layer, except for the surface layer (in summer). In the central area, there are multidirectional trends toward the warming in the upper 350-m layer and toward the cooling in the underlying layers. In the southern area, there is a gradual accumulation of heat in the layer of 300–400 m, which is most pronounced in the cold season; in the warm season, the heat loss is observed in the layer of 300–700 m.

The correlation was found that indicates the features of spatiotemporal variability of the fields of T_a , SST, and wind, the characteristics of atmospheric circulation, and the state of the atmospheric centers of action. These connections are expressed in terms of the 500 hPa geopotential height anomaly EOFs and climate indices. There are the effects of the first (especially in summer) and second (winter) modes of H_{500} variability on the spatiotemporal structure of the SSTA field in the Philippine Sea area. The zones of statistically significant correlations between the analyzed parameters and various climate indices are distinguished on the corresponding maps of isocorrelates and regression. These correlations are the highest with the Western Pacific (WP), Southern Oscillation (SOI), Atlantic Multidecadal Oscillation (AMO), Pacific trade wind (PTW), and East Pacific/North Pacific (EP/NP) indices.

FUNDING

The research was performed in the framework of the Governmental Assignment of Il'ichev Pacific Oceanological Institute (Far Eastern Branch, Russian Academy of Sciences), theme 0271-2019-0003 (state registration number AAAA-A17-117030110042-2).

REFERENCES

1. A. L. Bondarenko and V. V. Zhmur, "Nature and Forecasting Possibility of the El Niño/La Niña Phenomenon," *Meteorol. Gidrol.*, No. 11 (2004) [Russ. Meteorol. Hydrol., No. 11 (2004)].
2. S. Yu. Glebova, "Cyclonic Activity over the Pacific Rim in the Winter and Its Influence on Thermal Conditions of the Far Eastern Seas and Northwestern Pacific," *Meteorol. Gidrol.*, No. 10 (2011) [Russ. Meteorol. Hydrol., No. 10, **36** (2011)].
3. M. A. Danchenkov, "Currents in the Philippine Sea (Review)," in *Studying Oceanological Fields of the Indian and Pacific Oceans*, Ed. by N. P. Bulgakov (DVNTs AN SSSR, Vladivostok, 1977) [in Russian].
4. A. S. Krovnin, B. N. Kotenov, N. V. Mordasova, and G. P. Muryi, "Teleconnections in the Atmosphere and Ocean as a Basis of Long-term Fishery Prediction," *Trudy VNIRO*, No. 173 (2018) [in Russian].
5. A. D. Nelezin, "On Long-term Variability of Thermal State of Water in the Kuroshio EAZO," *Meteorol. Gidrol.*, No. 1 (1993) [Russ. Meteorol. Hydrol., No. 1 (1993)].
6. G. N. Panin, T. Yu. Vyruchalkina, and I. V. Solomonova, "Regional Climate Change in the Northern Hemisphere and Its Relationship with Circulation Indices," *Problemy Ekologicheskogo Monitoringa i Modelirovaniya Ekosistem*, No. 23 (2010) [in Russian].
7. V. V. Popova, "Modern Changes in Surface Air Temperature in Northern Eurasia: Regional Trends and Role of Atmospheric Circulation," *Izv. Akad. Nauk, Geogr.*, No. 6 (2009) [in Russian].
8. A. E. Rozhdestvenskii and G. A. Malyshev, "Evaluation of Heat Sources and Sinks in the Northern Hemisphere Atmosphere," *Uchenye Zapiski RGGMU. Meteorol.*, No. 45 (2016) [in Russian].
9. I. D. Rostov, E. V. Dmitrieva, N. I. Rudykh, and A. A. Vorontsov, "Climatic Changes in Thermal Conditions of Marginal Seas in the Western Pacific," *Meteorol. Gidrol.*, No. 3 (2020) [Russ. Meteorol. Hydrol., No. 3, **45** (2020)].

10. *The Pacific Ocean. Hydrology of the Pacific Ocean*, Ed. by A. D. Dobrovol'skii (Nauka, Moscow, 1968) [in Russian].
11. V. P. Tunegolovets, "Cyclone Activity over the Northwestern Pacific and Far Eastern Seas and Its Effect on the Active Layer," in *Far Eastern Seas of Russia, Book 1: Oceanological Research* (Nauka, Moscow, 2007) [in Russian].
12. A. V. Khokhlova and A. S. Lavrov, "Climatic Characteristics of Northern Hemisphere Tropospheric Jet Streams According to Radiosonde Observations," *Fundamental'naya i Prikladnaya Klimatologiya*, No. 3 (2018) [in Russian].
13. M. A. Balmaseda, K. E. Trenberth, and E. Kallen, "Distinctive Climate Signals in Reanalysis of Global Ocean Heat Content," *Geophys. Res. Lett.*, **40** (2013).
14. B. Bao and G. Ren, "Climatological Characteristics and Long-term Change of SST over the Marginal Seas of China," *Continental Shelf Res.*, **77** (2014).
15. Barnston A. G. and R. E. Livezey, "Classification, Seasonality, and Persistence of Low Frequency Atmospheric Circulation Patterns," *Mon. Wea. Rev.*, **115** (1987).
16. D. W. Behringer and Y. Xue, "Evaluation of the Global Ocean Data Assimilation System at NCEP: The Pacific Ocean," in *Eighth Symposium on Integrated Observing and Assimilation Systems for Atmosphere, Oceans, and Land Surface, AMS 84th Annual Meeting, Washington State Convention and Trade Center, Seattle, Washington* (2004).
17. A. Capotondi, A. T. Wittenberg, M. Newman, E. D. Lorenzo, J.-Y. Yu, P. Braconnot, J. Cole, B. Dewitte, B. Giese, E. Guilyardi, F. Jin, K. Karnauskas, B. Kirtman, T. Lee, N. Schneider, Y. Xue, and S. Yeh, "Understanding ENSO Diversity," *Bull. Amer. Meteorol. Soc.*, No. 6, **96** (2015).
18. D. R. Cayan, "Latent and Sensible Heat Flux Anomalies over the Northern Oceans: Driving the Sea Surface Temperature," *J. Phys. Oceanogr.*, No. 8, **22** (1992).
19. *Climate Change Monitoring Report 2018* (Japan Meteorological Agency (JMA), September 2019).
20. M. F. Cronin, N. A. Bond, J. T. Farrar, H. Ichikawa, S. Jayne, Y. Kawai, M. Konda, B. Qiu, L. Rainville, and H. Tomita, "Formation and Erosion of the Seasonal Thermocline in the Kuroshio Extension Recirculation Gyre," *Deep Sea Res. II*, **85** (2013).
21. B. J. Henley, J. Gergis, D. J. Karoly, S. Power, J. Kennedy, and C. Folland, "A Tripole Index for the Interdecadal Pacific Oscillation," *Climate Dynamics*, **45** (2015).
22. D. Hu and M. Cui, "The Western Boundary Current of the Pacific and Its Role in the Climate," *Chin. J. Oceanol. Limnol.*, No. 1, **9** (1991).
23. *Japan Meteorological Agency. Data of Oceanographic and Marine Meteorological Observations*, http://www.data.jma.go.jp/gmd/kaiyou/db/vessel_obs/data-report/html/index_e.html (Accessed September 21, 2020).
24. E. Kalnay, M. Kanamitsu, R. Kistler, W. Collins, D. Deaven, L. Gandin, M. Iredell, S. Saha, G. White, J. Woolen, Y. Zhu, M. Chelliah, W. Ebisuzaki, W. Higgins, J. Janowiak, K. C. Mo, C. Ropelewski, J. Wang, A. Leetma, R. Reynolds, R. Jenne, and D. Joseph, "The NCEP/NCAR 40-year Reanalysis Project," *Bull. Amer. Meteorol. Soc.*, No. 3, **77** (1996).
25. A. Kidwell, L. Han, Y.-H. Jo, and Y.-H. Yan, "Decadal Western Pacific Warm Pool Variability: A Centroid and Heat Content Study," *Sci. Rep.* (2017).
26. H. J. Kim, K. Hyeong, C. M. Yoo, B. K. Kim, K. H. Kim, J. W. Son, J. S. Kug, J. Y. Park, and D. Kim, "Impact of Strong El Niño Events (1997/98 and 2009/10) on Sinking Particle Fluxes in the 10°N Thermocline Ridge Area of the Northeastern Equatorial Pacific," *Deep-Sea Res. I*, **67** (2012).
27. Y.-O. Kwon, M. A. Alexander, N. A. Bond, C. Frankignoul, H. Nakamura, B. Qiu, and L. Thompson, "Role of the Gulf Stream and Kuroshio–Oyashio Systems in Large-scale Atmosphere–Ocean Interaction: A Review," *J. Climate*, No. 12, **23** (2010).
28. E. Oka, M. Ishii, T. Nakano, T. Suga, S. Kouketsu, M. Miyamoto, H. Nakano, B. Qiu, S. Sugimoto, and Y. Takatani, "Fifty Years of the 137°E Repeat Hydrographic Section in the Western North Pacific Ocean," *J. Oceanogr.*, **74** (2018).
29. C. H. O'Reilly and A. Czaja, "The Response of the Pacific Storm Track and Atmospheric Circulation to Kuroshio Extension Variability," *Quart. J. Roy. Meteorol. Soc.*, No. 686, **141** (2015).
30. R. W. Reynolds, N. A. Rayner, T. M. Smith, D. C. Stokes, and W. Wang, "An Improved in Situ and Satellite SST Analysis for Climate," *J. Climate*, No. 13, **15** (2002).
31. Y.-L. Wang and C.-R. Wu, "Enhanced Warming and Intensification of the Kuroshio Extension, 1999–2013," *Remote Sens.*, No. 101, **11** (2019).
32. Y.-L. Wang, C.-R. Wu, and S.-Y. Chao, "Warming and Weakening Trends of the Kuroshio during 1993–2013," *Geophys. Res. Lett.*, **43** (2016).
33. R. C. J. Wills, D. S. Battisti, C. Proistosescu, L. Thompson, D. Hartmann, and K. Armour, "Ocean Circulation Signatures of North Pacific Decadal Variability," *Geophys. Res. Lett.*, **46** (2019).
34. Z. Wu, C. Jiang, M. Conde, J. Chen, and B. Deng, "The Long-term Spatiotemporal Variability of Sea Surface Temperature in the Northwest Pacific and China Offshore," *Ocean Sci.*, No. 1, **16** (2020).